

Dissolved organic matter and inorganic mercury loadings favor novel methylators and fermentation metabolisms in oligotrophic sediments

Emily B. Graham^{1*}, Joseph E. Knelman², Rachel S. Gabor³, Shon Schooler⁴, Diane M. McKnight^{5,6,7}, Diana R. Nemergut^{5,8}

¹Biological Sciences Division, Pacific Northwest National Laboratory, Richland, WA, USA

²Joint Genome Institute, US Department of Energy, Walnut Creek, CA, USA

³Department of Geology and Geophysics, University of Utah, Salt Lake City, UT, USA

⁴Lake Superior National Estuarine Research Reserve, University of Wisconsin-Superior, Superior, WI, USA

⁵Institute for Arctic and Alpine Research, University of Colorado at Boulder, Boulder, CO, USA

⁶Civil Engineering Department, University of Colorado at Boulder, Boulder, CO, USA

⁷Environmental Studies Program, University of Colorado at Boulder, Boulder, CO, USA

⁸Biology Department, Duke University, Durham, NC, USA

Correspondence:

Emily B. Graham, emily.graham@colorado.edu

Biological Sciences Division, Pacific Northwest National Laboratory

902 Battelle Blvd.

Richland, WA, 99354, (509) 372-6049

Abstract.

Advances in genetics have allowed for greater investigation into the complex microbial communities mediating mercury methylation in the environment. In wetlands in particular, dissolved organic matter (DOM) may influence methylmercury production both through direct chemical interactions with mercury and through substrate effects on the environmental microbiome. We conducted microcosm experiments in two chemically disparate wetland environments (unvegetated and vegetated sediments) to examine the impact of DOM from leachate of local vegetation and inorganic mercury loadings on microbial community membership, metagenomic potential, DOM processing, and methylmercury production. We show that while DOM loadings impacted the microbiome in both environment types, sediment with high organic carbon content was more resistant than oligotrophic sediment to changes in microbial community structure and methylmercury production. We identify putative chemoorganotrophic methylators within the class *Clostridia* as primary community members associated with methylation rates in contrast to previous work focusing on microorganisms involved in sulfur, iron, and methane cycling. Metagenomic shifts toward fermentation, and secondarily iron metabolisms, as well as degradation of complex DOM indicated by fluorescence indices further support the involvement of rarely acknowledged biogeochemical pathways in mercury toxicity. We therefore propose that DOM addition in our system generates methylmercury production either 1) via direct methylation by fermenting bacteria or 2) via enhancing the bioavailability of simple carbon compounds for sulfate- and iron-reducing bacteria through breakdown of complex DOM. Our results demonstrate variation in sediment methylmercury production in response to DOM loading across geochemical environments and

- 23 provide a mechanistic framework for understanding linkages between environmental
- 24 microbiomes, carbon cycling, and mercury toxicity.

Introduction.

Mercury methylation in anoxic sediments is central to the bioaccumulation of mercury in plant and animal tissue (Benoit *et al.* 2003, Morel *et al.* 1998, Ullrich *et al.* 2001) and poses a significant environmental and human health concern in freshwater wetlands (Branfireun *et al.* 1999, Harmon *et al.* 2005, Jeremiason *et al.* 2006). Dissolved organic matter (DOM) has been a focus of geochemical investigations for decades, and both positive and negative interactions between DOM and mercury methylation – a microbial process – have been demonstrated under contrasting environmental conditions (Graham *et al.* 2013, Hsu-Kim *et al.* 2013, Ravichandran 2004). While the microbial mechanisms generating methylmercury are poorly understood, the recent discovery of the *hgcAB* gene cluster has allowed investigations into the microbial ecology of mercury cycling (Gilmour *et al.* 2013, Parks *et al.* 2013, Poulain and Barkay 2013, Smith *et al.* 2015). In particular, interactions between environmental microbiome (notably, newly identified methylating clades), DOM quantity and quality, and mercury methylation in natural systems remain an uncertainty in predicting hotspots of mercury toxicity in the environment (reviewed in Hsu-Kim *et al.* 2013, Podar *et al.* 2015).

Dissolved organic matter is comprised of various classes of organic compounds (primarily organic acids) with a wide range of molecular weights and aromaticities (Lambertsson and Nilsson 2006, Wetzel 1992). DOM concentrations are elevated in wetlands relative to other freshwater systems (>10 mg/L), and the humic fraction derived from plant leachate predominates. With respect to mercury cycling in wetlands, mercury methylation is impacted both by binding properties of the humic DOM fraction, resulting either in increased dissolution of inorganic mercury complexes or in physical inhibition of mercury bioavailability (Drexel *et al.* 2002, Haitzer *et al.* 2002, Waples *et al.* 2005), and by provisioning organic substrate for

microbial activity (Hsu-Kim *et al.* 2013, King *et al.* 2000, Lambertsson and Nilsson 2006). These effects may also vary with ambient geochemistry, as Graham *et al.* (2013) have demonstrated that sulfide concentrations and DOM aromaticity interact to influence MeHg production. The character of humic DOM can be assessed at scales relevant to microbial activity with fluorescence spectroscopy, which correlates changes in humic fluorescence relative to other portions of the optically-active DOM pool (Fellman *et al.* 2010).

Further, interactive effects of sediment microbiomes and DOM biogeochemistry are less well-resolved than other aspects of linkages between environmental geochemistry and mercury toxicity. Ecosystem carbon and nutrient status are known to influence microbial community membership (Graham *et al.* 2016a, Knelman *et al.* 2014), competitive interactions (Allison 2005, Fontaine *et al.* 2003, Stolpovsky *et al.* 2016), and metabolism (Graham *et al.* 2014, Graham *et al.* 2016b), with subsequent effects on pollutant cycling and ecosystem trophic status. In particular, numerous studies have shown regulation of freshwater microbial communities by DOM quantity or quality (Docherty *et al.* 2006, Forsström *et al.* 2013, Pernthaler 2013). For example, Eiler *et al.* (2003) demonstrated changes in microbial community membership in response to variation in dissolved organic carbon, and such changes in environmental microbiomes may alter ecosystem biogeochemical cycling (Graham *et al.* 2016b).

New work has increased knowledge on the microbiology of mercury methylation, expanding potential microorganisms mediating methylation beyond sulfate-reducing bacteria (Compeau and Bartha 1985, reviewed in Hsu-Kim *et al.* 2013), iron-reducing bacteria (Kerin *et al.* 2006) and methanogens (Hamelin *et al.* 2011). To date, all tested microorganisms containing the *hgcAB* gene cluster have been confirmed as methylators (Gilmour *et al.* 2013, Hsu-Kim *et al.* 2013). Gilmour *et al.* (2013) have identified five clades of putative methylators, including new

clades of syntrophic and *Clostridial* organisms. While research has provided insight into the abundance of these new organisms in mercury-contaminated landscapes (Bae *et al.* 2014, Hamelin *et al.* 2015, Liu *et al.* 2014a), many studies have continued to focus on the involvement of sulfate- (Liu *et al.* 2014b, Lu *et al.* 2016) and iron-reducing bacteria (Si *et al.* 2015) as well as methanogens (Yu *et al.* 2013) in mercury methylation. As such, the importance of organisms with alternative metabolisms in mercury methylation remain relatively unexplored. Resolving interactions between sediment microbiomes, environmental chemistry, and inorganic mercury complexes is thought to be central in understanding variation in methylation rates among natural systems (Gilmour *et al.* 2013, Hintelmann *et al.* 2000, Hsu-Kim *et al.* 2013).

Here, we examine the influence of plant leachate and inorganic mercury loadings on microbial methylmercury (MeHg) production in a contaminated freshwater estuary at the base of Lake Superior. We hypothesize that environmental biogeochemistry (in particular, DOM quantity and quality) exerts controls over mercury methylation rates through regulating total microbial activity and through influencing the abundance and metabolic diversity of mercury methylators. We test this hypothesis across chemically distinct oligotrophic versus high carbon (C) sediments associated with unvegetated and vegetated environments, using a microcosm experiment to monitor changes in sediment microbiomes, DOM chemical quality, and MeHg production in response to additions of leachate from overlying plant material and inorganic mercury. Our results suggest the involvement of novel methylating microorganisms with metabolisms that ferment recalcitrant organic matter in MeHg production, particularly within oligotrophic environments, an effect that may be imperative to understanding and mitigating human exposure to MeHg with increasing rates of anthropogenic eutrophication.

Methods.

Field site.

The St. Louis River Estuary is home to the largest U.S. port on the Great Lakes and covers roughly 12,000 acres of wetland habitat directly emptying into Lake Superior. Mining in the headwaters, industrial discharge in the port, and atmospheric deposition have left a legacy of mercury contamination in the sediment. We obtained sediment samples from wild rice (*Zizania palustris*, 46° 40.855' N, 91° 59.048' W) and unvegetated (46° 41.918' N, 92° 0.123' W) patches in Allouez Bay, which has high mercury concentrations relative to other areas of the estuary (data not shown). We also obtained wild rice plant matter from nearby Pokegama Bay (46.683448°N, 92.159261°W). Both habitats are clay influenced embayments that drain an alluvial clay plain created by deposition during the retreat of the last glaciation approximately 10,000 years BP.

Experimental design.

A total of 20 anoxic microcosms were constructed in September 2013 to investigate relationships between sediment microbiomes, DOM chemical quality, and mercury methylation. Sediment was obtained in 250-mL amber Nalgene bottles from the top 10 cm of sediment using a block sampling design described in the Supplemental Material. Leachate was extracted using 1 g dried, ground plant matter:20 mL of Nanopure water, filtered through Whatman 0.7 µm GFF filters (Whatman Incorporated, Florham Park, NJ, USA). Microcosms were constructed in 500-mL airtight glass mason jars and stored at room temperature in the dark in Mylar bags with oxygen-absorbing packets between subsampling. A full-factorial design was employed with two environments (vegetated and unvegetated sediment) and two treatments (plant leachate and Nanopure water). Each microcosm received 100 g wet sediment, and 250 mL solution consisting either of DOM at 100 mg/L and HgCl₂ at 20 mg/L in Nanopure water (DOM-amended

replicates) or solely of HgCl₂ at 20 mg/L in nanopure water (controls). Addition of HgCl₂ at high concentration negated initial differences in mercury and provided substrate for the duration of the experiment. Microcosms were incubated for 28 days, and subsamples of sediment and water were taken every seven days for analysis of sediment microbiomes and DOM characteristics. All sample processing was conducted in an anaerobic glovebox containing 85% N₂, 5% CO₂, and 10% H₂ gas mix at the USGS in Boulder, CO.

Sediment chemistry, extracellular enzyme activity, and mercury methylation.

Percent carbon and nitrogen, NO₃⁻/NO₂⁻, NH₄⁺, total particulate organic carbon (TPOC), total dissolved nitrogen (TDN), pH, and extracellular enzyme activities of β-1,4-glucosidase, β-1,4-N-acetylglucosaminidase, and acid phosphatase were determined on pre-incubation sediments, as described in the Supplemental Material. For total- and methylmercury analysis, initial (T0) and final (T4) subsamples were frozen at -70°C, freeze-dried, and sent on dry ice to the USGS Mercury Lab in Middleton, WI for analysis by aqueous phase ethylation, followed by gas chromatographic separation with cold vapor atomic fluorescence detection (Method 5A-8) and acid digestion (Method 5A-7). Mercury analyses were performed on 3 of 5 replicates for each environment and microcosm type. All other analyses were performed on 5 replicates, except for unvegetated controls beyond T0 (*n* = 4, one replicate destroyed during experiment).

Dissolved organic matter characteristics.

Water subsamples were collected at 7-day intervals (T0, T1, T2, T3, T4) to determine non-purgeable organic carbon (NPOC) concentration and specific UV absorbance at 254 nm (SUVA₂₅₄) as well characteristics of the optically active DOM pool (mostly associated with humic DOM fraction), as described in the Supplemental Material. We calculated the fluorescence index (FI) to determine the relative contribution of microbial vs. terrestrial matter to

the DOM pool, the humic index (HIX) to identify large aromatic compounds consistent with humic material, and the freshness index to determine the availability of labile carbon (reviewed in Fellman *et al.* 2010, Gabor *et al.* 2014a) using MATLAB software (2013a, The MathWorks, Natick, MA) according to Gabor *et al.* (2014b).

Microbial DNA extraction, 16S rRNA amplicon, and metagenomic shotgun sequencing.

DNA from each sediment subsample was extracted using the MO Bio Power Soil DNA Extraction kit (MO BIO Laboratories, Carlsbad, CA, USA), as described in Knelman *et al.* (2012). The region encoding the V4 fragment of the 16S rRNA gene was amplified with the primers 515F/806R, using the PCR protocol described by the Earth Microbiome Project (Supplemental Material, Caporaso *et al.* 2012). The final multiplexed DNA samples were sequenced at CU-Boulder (BioFrontiers Institute, Boulder, CO) on an Illumina MiSeq with the MiSeq Reagent Kit v2, 300 cycles (Illumina, Cat. # MS-102-2002) to generate 2 x 150-bp paired-end reads. Sequences are available at XXXXXX. In addition, 3 unvegetated DOM-amended replicates at T0 (before leachate additon) and T4 were sent to the Joint Genome Institute (JGI) for shotgun metagenomic sequencing on the Illumina HiSeq platform. Sequences are available at XXXXX.

Sequence analysis.

Partial 16S rRNA gene were filtered for sequence length and minimum quality score in the UPARSE pipeline (Edgar 2013) and OTUs were assigned using QIIME (Supplemental Material, Caporaso *et al.* 2010). Metagenomic shotgun sequences were assembled and classified against the protein families database (Pfam, Finn 2012), Clusters of Orthologous Groups of proteins (COG, Tatusov *et al.* 2003), and Kyoto Encyclopedia of Genes and Genomes (KEGG, Kanehisa and Goto 2000) by JGI via the IMG database pipeline (Markowitz *et al.* 2012).

In addition, 46 of 52 genomes identified by Parks *et al.* (2013) were represented by complete or partial 16S rRNA gene sequences in the NCBI GenBank database (Benson *et al.* 2013), spanning all clades of methylators. We used two different approaches to determine methylator relative abundance and community structure. To determine relative abundance, we combined available methylating sequences with generated sequences and re-performed *de novo* OTU-picking. We then identified OTUs containing known methylator sequences as potential methylators. Because of high *Deltaproteobacteria* abundance, many closely-related methylator sequences may have clustered with non-methylating *Deltaproteobacteria* in this approach. Thus, to examine methylator community structure, we created a database of known methylator sequences and performed closed-reference OTU-picking in QIIME against this database. In addition, a BLAST database was constructed from all *hgcA* and *hgcB* gene sequences available in GenBank. A BLASTX search was conducted against this database to identify taxonomic affiliation of methylators in our samples; however, our query resulted in no matches, likely due to inadequate sequencing depth.

Statistical analysis.

All analyses, unless otherwise noted, were conducted using the *R* software platform. Shapiro-Wilk tests were used to verify normality and assess the appropriateness of parametric vs. non-parametric tests. Comparisons of initial conditions across environments (T0, sediment geochemistry, extracellular enzyme activity, and DNA quantity) were completed using paired unequal variance Student's *t*-tests. MeHg production was calculated by subtracting T0 from T4 MeHg concentrations; values below detection limit were assigned the detection limit as a value for a conservative estimate of change. MeHg production in DOM-amended vs. control microcosms within each environment as well as across environment types were compared using

paired unequal variance Student's *t*-tests. Changes in DOM indices (FI, freshness, HIX) through time (T0-T4) in each sample group were assessed with linear and quadratic regressions. DOM samples with SUVA₂₅₄ >7 were removed due to fluorescence interference from inorganic molecules. Comparisons of DOM indices between data subsets were conducted with Student's *t*-tests.

Microbial community dissimilarity matrices based on 16S rRNA sequences were constructed using the weighted UniFrac method (Lozupone *et al.* 2011) in QIIME. We performed analysis using the full community and within the methylating community. To examine the relative abundance of our methylating OTUs, we removed OTUs with less than eight total occurrences (bottom quartile) in our 91 subsamples to limit artifacts from sequencing errors. Alpha diversity for each sample was assessed using the PD whole tree metric in QIIME. The relative abundance of methylators was compared between DOM-amended and control microcosms within each environment at T0 and T4 using paired unequal variance Student's *t*-tests.

Changes in community membership through time (T0-T4) were assessed with ANOSIM in QIIME. Differences in alpha diversity at T0 were assessed using paired unequal variance Student's *t*-tests. Relative abundances of major clades were assessed between vegetated and unvegetated environments at T0 and changes in clades through time (T0-T4) were assessed using non-parametric Kruskal-Wallis tests. SIMPER analysis was conducted using the 'vegan package' to identify OTUs driving community dissimilarity between T0 and T4 in microcosms receiving DOM. Correlations between methylating clades that exhibited significant changes (Kruskal-Wallis, T0-T4), HIX, and MeHg production were assessed at T4 using Pearson's Correlation,

grouping DOM-amended and control microcosms within each environment in a single analysis to provide sufficient variation.

Upregulation of COGs, Pfams, and KEGG pathways in at T4 relative to T0 were evaluated using binomial tests. Upregulated targets (FDR-corrected $P < 0.01$) were examined for correlations with HIX and MeHg production at T4 with Pearson's Correlation.

Results.

Ambient geochemistry and microbiology.

NH_4^+ , TPOC, TDN, percent C, percent nitrogen (N), extracellular enzyme activities, and ambient total- and MeHg concentrations were significantly higher within vegetated sediment compared to unvegetated sediment (Table 1). pH did not differ, and $\text{NO}_3^-/\text{NO}_2^-$ concentrations were below the detection level in both environments. The unvegetated environment was extremely oligotrophic, with low concentrations of sediment C and N, and both vegetated and unvegetated environments appeared to be N-limited (C:N 16.43 and 20.06). DNA concentration, enzyme activities, and mercury concentrations were an order of magnitude higher within the vegetated environment (Table 1).

Microbial community structure was significantly different between the two environments (ANOSIM, $P = 0.001$, $R = 1.00$), though alpha diversity did not differ and major phyla were similar (Table 1). The relative abundance of methylators was higher in the vegetated environment (t -test, $P = 0.02$), and the structure of potential methylators within microbial communities also differed between environments (ANOSIM, $P = 0.001$, $R = 0.99$).

Microbiome response to HgCl_2 and DOM addition.

Over the course of the incubation, microcosms with vegetated, high-C sediment produced over ten times more MeHg than unvegetated sediment microcosms, regardless of DOM

amendment (t -test, control $P = 0.04$, DOM $P = 0.01$, Figure 1). In addition, mercury methylation was significantly enhanced by DOM addition within the unvegetated nutrient-poor environment with roughly two to four times more production in microcosms receiving DOM as compared to controls (t -test, $P = 0.04$, Figure 1). However, DOM addition did not stimulate significantly more MeHg production than control replicates in the vegetated environment (t -test, $P > 0.05$, Figure 1).

Community membership changed through time in vegetated and unvegetated environments amended with DOM (ANOSIM T0-T4, veg.: $P = 0.001$ $R = 0.40$, unveg.: $P = 0.001$ $R = 0.43$, Figure S1A and B), but not in controls (veg.: $P = 0.02$, $R = 0.19$, unveg.: $P > 0.05$, Figure S1C and D). At T4, communities in unvegetated microcosms amended with DOM were different than controls (ANOSIM, $P = 0.01$, $R = 0.54$), while structure in vegetated sediment microcosms only weakly differed between control and DOM-amended groups ($P = 0.04$, $R = 0.22$). When examining only potential methylators, the relative abundance of methylators was significantly greater in the DOM-amended microcosms versus controls for each environment at T4 (Figure 2A, t -test, veg.: $P = 0.03$, unveg.: $P = 0.05$). However, for both environments, there were no significant changes in community membership within methylating clades through time (ANOSIM, T0-T4, $P > 0.05$). This result was not unexpected given our small sample sizes (methylator OTUs contained less than 1% of sequences).

Variation in community membership in response to DOM addition was partially generated by an increase in *Clostridia* (Kruskal-Wallis, veg.: $P = 0.001$, unveg.: $P = 0.006$, Figure 2B) and a decrease in *Deltaproteobacteria* (Kruskal-Wallis, veg.: $P = 0.12$, unveg.: $P = 0.005$, Figure 2B) in both environments. In particular, *Clostridia* abundances increased by 3-fold and 10-fold, respectively in vegetated and unvegetated environments, driven by increases in

nearly all families of *Clostridia*. These shifts were mirrored within our subset of data containing only suspected methylators (Figure 2C), which showed distinct (non-significant) trends for increases in *Clostridia* and decreases in *Deltaproteobacteria* in response to DOM addition in both environments.

Changes in the methylating community were more evident at finer taxonomic levels. One family of *Clostridia* (*Peptococcaceae*), sharply increased with DOM addition (Kruskal-Wallis, veg.: $P = 0.09$, unveg.: $P = 0.02$, Figure 2D). These changes were driven by two closely related methylating OTUs (Kruskal-Wallis, *Dehalobacter restrictus* veg.: $P = 0.04$, and *Syntrophobotulus glycolicus*, unveg.: $P = 0.001$) grouped in a single genus by our classification system (*Dehalobacter_Syntrophobotulus*, Kruskal-Wallis, veg.: $P = 0.03$, unveg.: $P = 0.0009$, Figure S2). Increases in *Clostridia* (t -test, $P = 0.002$), *Peptococcaceae* (t -test, $P = 0.009$), *Dehalobacter restrictus* (t -test, $P = 0.004$), and *Syntrophobotulus glycolicus* (t -test, $P = 0.007$) as well a trend for decreases in *Deltaproteobacteria* (t -test, $P = 0.09$) were also reflected in metagenomic data (Figure 3D).

SIMPER analysis of 16S rRNA genes associated with methylator taxonomy in unvegetated DOM-amended microcosms indicated that two OTUs, in *D.r restrictus* (increase) and in *Geobacter* (decrease), significantly contributed to community differences between T0 and T4 ($P < 0.05$, Table S1). This was reflective of broader changes in the full community, in which 22.9% of 175 SIMPER-identified OTUs belonged to *Clostridia* (increased from avg. 0.78 OTUs/sample to avg. 17.20 OTUs/sample, Table S3) while 8% belonged to *Deltaproteobacteria* (decreased from avg. 8.5 OTUs/sample to 7.4 OTUs/sample, Table S2).

In total, 7,150 KEGG pathways, 84 COGs, and 79 Pfams were upregulated at T4 relative to T0 in unvegetated DOM-amended microcosms. Upregulated KEGG pathways, COGs, and

Pfams with the greatest levels of expression are presented in Figure 3A, B and C, respectively. All upregulated targets denoted enhanced expression of glycosyltransferases, among other pathways involved in DOM oxidation and in iron and nitrate reduction.

Changes in DOM chemistry.

Details of DOM quantity and quality changes are presented in the Supplemental Material and regression statistics are presented in Table 2. Control microcosms for both environments displayed increasing NPOC concentrations (Figure S3A), while total fluorescence (Figure S3C) and the ratio of fluorescence to NPOC concentration (Figure S3E) displayed non-significant trends or decreased. Within DOM-amended microcosms, vegetated microcosms displayed a decrease in NPOC concentration (Figure S3B), while unvegetated microcosms had stable NPOC content (Figure S3B). Total fluorescence remained stable in both environments (Figure S3D). The ratio of fluorescence-to-NPOC was variable through time and did not statistically change in either environment (Figure S3F).

DOM fluorescence indices displayed notable changes through time. In the vegetated environment, FI remained stable in DOM-amended microcosms at a low value, indicating plant-derived DOM, and rose in controls indicating greater relative contribution of microbial vs. abiotic processing (Figure 4A and B). In contrast, in the vegetated environment, HIX increased in both control and DOM-amended microcosms indicating processing of more labile vs. recalcitrant DOM (Figure 4C and D). This increase in HIX corresponded with decrease in freshness (Figure 4E and F), further supporting our interpretation. In the unvegetated environment, DOM-amended microcosms (but not controls) increased in FI (Figure 4A and B) denoting progressively microbial DOM sources. There was no change in HIX (Figure 4C and D)

suggesting equal processing of labile vs. recalcitrant DOM. Freshness varied non-linearly in DOM-amended but not control microcosms (Figure 4E and F).

Across environment types, HIX was significantly higher in vegetated microcosms (t -test, DOM-amended: $P < 0.0001$, control: $P = 0.005$). FI and freshness were higher in unvegetated DOM-amended microcosms than in vegetated DOM-amended microcosms (t -test, FI: $P = 0.0006$, freshness: $P < 0.0001$) but did not differ across control microcosms (FI: $P = 0.76$, freshness: $P = 0.12$).

Correlation of microbiome, DOM characteristics, and MeHg production.

Given the apparent shift in community structure towards *Clostridia*, and *Peptococcaceae* (putative chemoorganotrophic methylators) in particular, we examined correlations of this family with the proportion of complex organic matter (HIX) and MeHg production within each environment. We focused on HIX because this index changed consistently and reflected portions of recalcitrant carbon substrate pools utilized by the organisms we identified. Because we only calculated MeHg production at the conclusion of the incubation, we analyzed these correlations at T4 and grouped DOM-amended and control replicates within each environment to provide sufficient variation and sample size. *Peptococcaceae* was negatively correlated with HIX and positively correlated with MeHg production in unvegetated microcosms (Pearson ($n = 6$), HIX: $P = 0.001$, $r = -0.96$, MeHg: $P = 0.03$, $r = 0.81$). *Peptococcaceae* abundance in vegetated microcosms did not correlate with HIX ($P = 0.20$) or MeHg production ($P = 0.45$).

Finally, despite low statistical power ($n = 3$), we observed notable trends ($P < 0.10$) between key metabolic pathways and HIX (Table 3). In particular, COGs classified as: Glycosyltransferase, Glycosyltransferases involved in cell wall biogenesis, Transcriptional regulator, HD-GYP domain, Glycosyltransferases - probably involved in cell wall biogenesis,

Beta-galactosidase/beta-glucuronidase, Nitroreductase, and Thiamine biosynthesis enzyme ThiH and related uncharacterized enzymes; and Pfams classified as: WD40-like Beta Propeller Repeat, Glycosyl transferase family 2, Radical SAM superfamily, HD domain, Doubled CXXCH motif, and SusD family displayed significant correlations with HIX at the $P < 0.10$ level. Only Pfam PF00593, TonB dependent receptor, correlated with MeHg production ($P < 0.001$, $r = -1.00$, Table 2).

Discussion.

Mercury methylation across environments.

Geochemical and microbial characteristics varied across environments, resulting in differential patterns of MeHg production. Within the vegetated high-C environment, DOM and HgCl₂ addition did not influence the sediment microbiome or MeHg production to the same extent as within the unvegetated environment (Figure 1, Figure S1). Given high ratios of C:N, high OC content, and low NO₃⁻ concentrations in our vegetated sediment (Table 1), N-limitation may have mitigated MeHg production in vegetated environments relative to the unvegetated environment (Taylor and Townsend 2010), which had substantially lower concentrations of all measured C and nutrient concentrations. Both ambient MeHg levels and MeHg production were an order of magnitude higher in the vegetated environment, supporting other findings that plant-microbe interactions inherently facilitates MeHg production (Roy *et al.* 2009, Windham-Myers *et al.* 2014, Windham - Myers *et al.* 2009). Indeed, the vegetated environment displayed higher ambient DNA concentration, enzyme activities, and methylator abundance, underlying a higher *in situ* rate of biological activity and MeHg production.

By contrast, the oligotrophic unvegetated environment experienced a dramatic increase in MeHg production (Figure 1) in response to DOM and HgCl₂ addition that correlated with

changes in the sediment microbiome (Figure 2 and 3, Figure S1). Carbon limitation has been widely demonstrated as a constraint on microbial activity (Bradley *et al.* 1992, Brooks *et al.* 2005, Wett and Rauch 2003); thus, DOM addition may bolster MeHg production in C-limited ecosystem from resultant increases in microbial activity. In our system, MeHg production in the unvegetated environment was possibly also constrained by low *in situ* rates of microbial activity and by low N concentration, and MeHg production in response to DOM stimulus never increased to vegetated levels. Importantly, DOM enhanced the relative abundance of putative methylators within the microbiome in both environments, indicating that mercury methylation rates may be dually influenced by the sediment microbiome and by organic matter.

Microbiome response to HgCl₂ and DOM addition.

Our results bolster support for recent work demonstrating preferential organic degradation by *Clostridial* fermentation over organic matter processing by *Deltaproteobacteria* (Reimers *et al.* 2013) and provide evidence for the involvement of this clade in MeHg production. Within both environments, DOM amendment altered the sediment microbiome, with structural shifts denoting an increase in *Clostridia* and decrease in *Deltaproteobacteria*. Unvegetated microcosms displayed greater changes in these clades, supporting a greater role for environmental filtering by DOM within oligotrophic environments (Barberán *et al.* 2012, Stegen *et al.* 2012). *Clostridia* are obligate anaerobes with the ability to produce labile carbon compounds via fermentation of recalcitrant organic matter (Reimers *et al.* 2013, Ueno *et al.* 2016). Recent work has shown organic carbon degradation via *Clostridial* fermentation to operate at comparable rates to more energetically favorable carbon processing pathways (Reimers *et al.* 2013). Moreover, organic acids (*e.g.*, lactate and acetate) produced through these pathways can be subsequently utilized as a carbon source by sulfate- and iron- reducing

Deltaproteobacteria (Guerrero-Barajas *et al.* 2011, Reimers *et al.* 2013, Zhao *et al.* 2008).

Importantly, microbiome changes were mirrored when examining putative methylators independently. Specifically, *Deltaproteobacteria* and *Clostridia*, respectively, were the most abundant methylating organisms at the end of the incubation in all experimental groups except vegetated controls.

In unvegetated sediments, although no methylating pathways were identified, metagenomic analyses indicated upregulation of carbon, and secondarily, iron metabolisms at the incubation conclusion, supporting a role for microbial carbon and iron cycling in mercury methylation (Gilmour *et al.* 2013, Hamelin *et al.* 2011, Kerin *et al.* 2006, Podar *et al.* 2015). Carbon metabolisms were the primary upregulated KEGG category (Figure 3A), and several COG pathways and Pfams indicated overexpression of glycosyltransferases that convert starches, sugars, and nitroaromatics into a wide range of compounds (Bowles *et al.* 2005, Ramli *et al.* 2015, Figure 3B and C). Glycosyltransferases can also modify plant-derived secondary metabolites and produce toxins in *Clostridia* (Bowles *et al.* 2005, Busch *et al.* 2000, Jank *et al.* 2015). Further, the upregulation of Beta-galactosidase/beta-glucuronidase (lactose to galactose/glucose, Martini *et al.* 1987), sugar phosphate isomerase/epimerases (sugar metabolism, Yeom *et al.* 2013), and lactoylglutathione lyase (detoxification for methyglyoxal fermentation byproduct, Inoue and Kimura 1995) and the SusD family (glycan binding, Martens *et al.* 2009) provide additional evidence increases in fermentation processes in response to DOM addition. Intercellular signaling (HD domain, Aravind and Koonin 1998, HD-GYP domain, Galperin *et al.* 1999, FOG: PAS/PAC domain, Taylor and Zhulin 1999) and competitive (RHS repeat, Koskiniemi *et al.* 2013) processes were also upregulated, possibly indicating more stressful environmental conditions; and upregulation of TonB dependent receptors (Moeck and

Coulton 1998), amidohydrolase (Seibert and Raushel 2005), and NRAMP (Cellier *et al.* 1995) suggest a secondary importance of iron processing and/or transport of large organic compounds across cellular membranes. Finally, our results provide a possible genetic mechanism connecting iron, sulfur, carbon, and mercury cycling, as the radical SAM superfamily, which facilitates methyl transfers via the use of a [4Fe-S]⁺ cluster (Booker and Grove 2010), was upregulated at the end of the incubation. In total, the metabolic potential of the sediment microbiome indicates changes in carbon and iron metabolisms and in microbial stress responses, supporting past work that suggests a linkage between mercury methylation and these factors (Gilmour *et al.* 2013, Hamelin *et al.* 2011, Hsu-Kim *et al.* 2013, Kerin *et al.* 2006, Podar *et al.* 2015).

Lastly, at high taxonomic resolution in both environments, DOM addition increased the proportion of methylating organisms classified as *Peptococcaceae* within *Clostridia*, despite drastic differences in sediment chemistry (Figure 2D). Specifically, the two OTUs displaying the greatest change are thought to generate energy via organohalide respiration (*D. restrictus*) and fermentative oxidation of organic matter (*S. glycolicus*, also capable of syntrophy, Han *et al.* 2011, Stackebrandt 2014). The relative abundance of *Peptococcaceae* was positively correlated with MeHg production in the unvegetated environment, and other methylating organisms did not increase in abundance, as would be expected if the activity of these organisms was enhanced by DOM addition.

Associations between microbiology, DOM processing, and MeHg production.

The processing of proportionally more labile organic matter would be expected to result in decreases in DOM freshness and increases in HIX. However, our results suggest substantial contributions of recalcitrant organic matter processing within the unvegetated environment (but not the vegetated environment which followed expectations). In unvegetated microcosms

(controls and DOM-amended), HIX did not rise through time indicating recalcitrant matter processing (Figure 4C and D). Further, DOM-amended unvegetated microcosms, which experienced pronounced changes in the sediment microbiome and high MeHg production, HIX was significantly lower than in all other experimental groups (ANOVA, $P < 0.0001$, all Tukey HSD $P < 0.0001$). While most microorganisms preferentially degrade labile C sources, the degradation of recalcitrant organic matter can contribute substantially to aquatic carbon cycling (McLeod *et al.* 2011). DOM-amended unvegetated microcosms also exhibited large increases in microbially-derived DOM (FI) through time, demonstrating a noticeable contribution of microbial activity to the DOM pool (Figure 4A).

The abundance of methylating *Peptococcaceae* in unvegetated microcosms negatively correlated with HIX, denoting an apparent contribution of these members or co-occurring community members to DOM processing, but the mechanisms behind these shifts remain unclear. Metabolism of recalcitrant organic matter by fermenting organisms may influence mercury methylation via direct and indirect mechanisms. Members of *Clostridia* can generate MeHg themselves, and *Clostridial* degradation of recalcitrant organic matter can also produce bioavailable carbon substrates for sulfate- and iron- reducing organisms that produce MeHg (Reimers *et al.* 2013). Regardless of the mechanism, *Clostridial* DOM processing appears to significantly contribute to MeHg production within oligotrophic sediments, and metagenomic analysis elucidates key metabolic pathways in recalcitrant organic matter processes in our system.

For example, both COG and Pfam glycosyltransferases were negatively correlated with HIX, suggesting the involvement of these enzymes in fermenting starches, sugars, and nitroaromatics. Cellular signaling mechanisms (HD-GYP/HD domains) and nitroreductase, were

also negatively correlated with HIX, indicating roles for stress and nitrate reduction in changes in community carbon cycling. As well, a negative correlation between HIX, and the radical SAM superfamily provides a possible mechanistic linkage between methyl transfers and recalcitrant organic matter processing. Conversely, Beta-galactosidase/beta-glucuronidase, Thiamine biosynthesis enzyme (ThiH), and the SusD family were positively correlated with HIX, indicating a co-association with labile C processing rather than recalcitrant organic matter. Only one abundant Pfam – a TonB dependent receptor, signaling enzyme that may be involved in iron cycling (Moeck and Coulton 1998) – and no COGs was correlated with MeHg production. Although our results do not provide a direct linkage between metabolic pathways and mercury methylation, it is notable that no pathways associations involve sulfate-reducing or methanogenic methylators.

Conclusions.

Microbiome shifts towards fermentation pathways, increases in chemoorganotrophic *Clostridia*, degradation of recalcitrant organic matter, and production of MeHg within oligotrophic environments begin to elucidate the microbial ecology of mercury methylation. Importantly, our results indicate that microbial clades not typically considered can exert controls over MeHg production in oligotrophic environments. *Clostridia* thrive in a variety of anoxic environments from wastewater effluent (Wang *et al.* 2003) to the human gut (Mahowald *et al.* 2009), and our work supports the potential for mercury methylation across a broader range of ecological niches than historically considered (Gilmour *et al.* 2013, Podar *et al.* 2015).

While we observed evidence for changes in the microbiome of both high-C and nutrient-poor sediment, the more oligotrophic environment showed greater responses in the sediment microbiome and in mercury methylation to the addition of DOM, an important insight given

increasing risks of anthropogenic eutrophication. Taken together, our insights highlight vital new aspects of the microbiome in generating MeHg and emphasize the importance of exploring microbial physiology not typically associated with methylating organisms in enhancing mercury toxicity.

Acknowledgements.

This work was supported by EPA STAR and NOAA NERRS fellowships to EBG and a JGI CSP grant to DRN. We also acknowledge support from the US Department of Energy (DOE), Office of Biological and Environmental Research (BER), as part of Subsurface Biogeochemical Research Program's Scientific Focus Area (SFA) at the Pacific Northwest National Laboratory (PNNL). PNNL is operated for DOE by Battelle under contract DE-AC06-76RLO 1830. We thank Alan Townsend, Teresa Bilinski, Deb Repert, Dick Smith, Steve Schmidt, Sharon Collinge, Garrett Rue, Jess Ebert, Alexis Templeton, and the LSNERR staff for valuable support and feedback during this project.

Literature Cited.

- Allison SD (2005). Cheaters, diffusion and nutrients constrain decomposition by microbial enzymes in spatially structured environments. *Ecology Letters* **8**: 626-635.
- Aravind L, Koonin EV (1998). The HD domain defines a new superfamily of metal-dependent phosphohydrolases. *Trends in biochemical sciences* **23**: 469-472.
- Bae H-S, Dierberg FE, Ogram A (2014). Syntrophs Dominate Sequences Associated with the Mercury Methylation-Related Gene *hgcA* in the Water Conservation Areas of the Florida Everglades. *Applied and environmental microbiology* **80**: 6517-6526.
- Barberán A, Bates ST, Casamayor EO, Fierer N (2012). Using network analysis to explore co-occurrence patterns in soil microbial communities. *The ISME journal* **6**: 343-351.
- Benoit J, Gilmour C, Heyes A, Mason R, Miller C (2003). Geochemical and biological controls over methylmercury production and degradation in aquatic ecosystems. *ACS symposium series* **835**: 262-297.
- Benson DA, Cavanaugh M, Clark K, Karsch-Mizrachi I, Lipman DJ, Ostell J *et al* (2013). GenBank. *Nucleic acids research* **41**: D36-D42.
- Booker SJ, Grove TL (2010). Mechanistic and functional versatility of radical SAM enzymes. *F1000 Biol Rep* **2**: 52.
- Bowles D, Isayenkova J, Lim E-K, Poppenberger B (2005). Glycosyltransferases: managers of small molecules. *Current opinion in plant biology* **8**: 254-263.
- Bradley P, Fernandez Jr M, Chapelle F (1992). Carbon limitation of denitrification rates in an anaerobic groundwater system. *Environmental science & technology* **26**: 2377-2381.
- Branfireun BA, Roulet NT, Kelly C, Rudd JW (1999). In situ sulphate stimulation of mercury methylation in a boreal peatland: Toward a link between acid rain and methylmercury contamination in remote environments. *Global Biogeochemical Cycles* **13**: 743-750.
- Brooks PD, McKnight D, Elder K (2005). Carbon limitation of soil respiration under winter snowpacks: potential feedbacks between growing season and winter carbon fluxes. *Global Change Biology* **11**: 231-238.
- Busch C, Hofmann F, Gerhard R, Aktories K (2000). Involvement of a conserved tryptophan residue in the UDP-glucose binding of large clostridial cytotoxin glycosyltransferases. *Journal of Biological Chemistry* **275**: 13228-13234.
- Caporaso JG, Kuczynski J, Stombaugh J, Bittinger K, Bushman FD, Costello EK *et al* (2010). QIIME allows analysis of high-throughput community sequencing data. *Nature methods* **7**: 335-336.

Caporaso JG, Lauber CL, Walters WA, Berg-Lyons D, Huntley J, Fierer N *et al* (2012). Ultra-high-throughput microbial community analysis on the Illumina HiSeq and MiSeq platforms. *The ISME journal* **6**: 1621-1624.

Cellier M, Prive G, Belouchi A, Kwan T, Rodrigues V, Chia W *et al* (1995). Nramp defines a family of membrane proteins. *Proceedings of the National Academy of Sciences* **92**: 10089-10093.

Compeau G, Bartha R (1985). Sulfate-reducing bacteria: principal methylators of mercury in anoxic estuarine sediment. *Applied and environmental microbiology* **50**: 498-502.

Docherty KM, Young KC, Maurice PA, Bridgham SD (2006). Dissolved organic matter concentration and quality influences upon structure and function of freshwater microbial communities. *Microbial Ecology* **52**: 378-388.

Drexel RT, Haitzer M, Ryan JN, Aiken GR, Nagy KL (2002). Mercury (II) sorption to two Florida Everglades peats: Evidence for strong and weak binding and competition by dissolved organic matter released from the peat. *Environmental science & technology* **36**: 4058-4064.

Edgar RC (2013). UPARSE: highly accurate OTU sequences from microbial amplicon reads. *Nature methods* **10**: 996-998.

Eiler A, Langenheder S, Bertilsson S, Tranvik LJ (2003). Heterotrophic bacterial growth efficiency and community structure at different natural organic carbon concentrations. *Applied and Environmental Microbiology* **69**: 3701-3709.

Fellman JB, Hood E, Spencer RG (2010). Fluorescence spectroscopy opens new windows into dissolved organic matter dynamics in freshwater ecosystems: A review. *Limnology and Oceanography* **55**: 2452-2462.

Finn RD (2012). Pfam: the protein families database. *Encyclopedia of Genetics, Genomics, Proteomics and Bioinformatics*.

Fontaine S, Mariotti A, Abbadie L (2003). The priming effect of organic matter: a question of microbial competition? *Soil Biology and Biochemistry* **35**: 837-843.

Forsström L, Roiha T, Rautio M (2013). Responses of microbial food web to increased allochthonous DOM in an oligotrophic subarctic lake. *Aquatic microbial ecology* **68**: 171-184.

Gabor RS, Baker A, McKnight DM, Miller MP (2014a). Fluorescence Indices and Their Interpretation. *Aquatic Organic Matter Fluorescence*: 303.

Gabor RS, Eilers K, McKnight DM, Fierer N, Anderson SP (2014b). From the litter layer to the saprolite: Chemical changes in water-soluble soil organic matter and their correlation to microbial community composition. *Soil Biology and Biochemistry* **68**: 166-176.

Galperin MY, Natale DA, Aravind L, Koonin EV (1999). A specialized version of the HD hydrolase domain implicated in signal transduction. *Journal of molecular microbiology and biotechnology* **1**: 303-305.

Gilmour CC, Podar M, Bullock AL, Graham AM, Brown SD, Somenahally AC *et al* (2013). Mercury methylation by novel microorganisms from new environments. *Environmental science & technology* **47**: 11810-11820.

Graham AM, Aiken GR, Gilmour CC (2013). Effect of dissolved organic matter source and character on microbial Hg methylation in Hg-S-DOM solutions. *Environmental science & technology* **47**: 5746-5754.

Graham E, Crump AR, Resch CT, Fansler S, Arntzen E, Kennedy D *et al* (2016a). Coupling spatiotemporal community assembly processes to ecosystem function. PeerJ Preprints.

Graham EB, Wieder WR, Leff JW, Weintraub SR, Townsend AR, Cleveland CC *et al* (2014). Do we need to understand microbial communities to predict ecosystem function? A comparison of statistical models of nitrogen cycling processes. *Soil Biology and Biochemistry* **68**: 279-282.

Graham EB, Knelman JE, Schindlbacher A, Siciliano S, Breulmann M, Yannarell A *et al* (2016b). Microbes as engines of ecosystem function: When does community structure enhance predictions of ecosystem processes? *Frontiers in microbiology* **7**.

Guerrero-Barajas C, Garibay-Orijel C, Rosas-Rocha LE (2011). Sulfate reduction and trichloroethylene biodegradation by a marine microbial community from hydrothermal vents sediments. *International Biodeterioration & Biodegradation* **65**: 116-123.

Haitzer M, Aiken GR, Ryan JN (2002). Binding of mercury (II) to dissolved organic matter: the role of the mercury-to-DOM concentration ratio. *Environmental Science & Technology* **36**: 3564-3570.

Hamelin S, Amyot M, Barkay T, Wang Y, Planas D (2011). Methanogens: principal methylators of mercury in lake periphyton. *Environmental science & technology* **45**: 7693-7700.

Hamelin S, Planas D, Amyot M (2015). Mercury methylation and demethylation by periphyton biofilms and their host in a fluvial wetland of the St. Lawrence River (QC, Canada). *Science of the Total Environment* **512**: 464-471.

Han C, Mwirichia R, Chertkov O, Held B, Lapidus A, Nolan M *et al* (2011). Complete genome sequence of Syntrophobotulus glycolicus type strain (FIGlyRT). *Standards in genomic sciences* **4**: 371.

Harmon S, King J, Gladden J, Chandler GT, Newman L (2005). Mercury body burdens in *Gambusia holbrooki* and *Erimyzon sucetta* in a wetland mesocosm amended with sulfate. *Chemosphere* **59**: 227-233.

Hintelmann H, Keppel - Jones K, Evans RD (2000). Constants of mercury methylation and demethylation rates in sediments and comparison of tracer and ambient mercury availability. *Environmental toxicology and chemistry* **19**: 2204-2211.

Hsu-Kim H, Kucharzyk KH, Zhang T, Deshusses MA (2013). Mechanisms regulating mercury bioavailability for methylating microorganisms in the aquatic environment: a critical review. *Environmental science & technology* **47**: 2441-2456.

Inoue Y, Kimura A (1995). Methylglyoxal and regulation of its metabolism in microorganisms. *Advances in microbial physiology* **37**: 177.

Jank T, Belyi Y, Aktories K (2015). Bacterial glycosyltransferase toxins. *Cellular microbiology* **17**: 1752-1765.

Jeremiason JD, Engstrom DR, Swain EB, Nater EA, Johnson BM, Almendinger JE *et al* (2006). Sulfate addition increases methylmercury production in an experimental wetland. *Environmental science & technology* **40**: 3800-3806.

Kanehisa M, Goto S (2000). KEGG: kyoto encyclopedia of genes and genomes. *Nucleic acids research* **28**: 27-30.

Kerin EJ, Gilmour C, Roden E, Suzuki M, Coates J, Mason R (2006). Mercury methylation by dissimilatory iron-reducing bacteria. *Applied and environmental microbiology* **72**: 7919-7921.

King JK, Kostka JE, Frischer ME, Saunders FM (2000). Sulfate-reducing bacteria methylate mercury at variable rates in pure culture and in marine sediments. *Applied and Environmental Microbiology* **66**: 2430-2437.

Knelman JE, Legg TM, O'Neill SP, Washenberger CL, González A, Cleveland CC *et al* (2012). Bacterial community structure and function change in association with colonizer plants during early primary succession in a glacier forefield. *Soil Biology and Biochemistry* **46**: 172-180.

Knelman JE, Schmidt SK, Lynch RC, Darcy JL, Castle SC, Cleveland CC *et al* (2014). Nutrient addition dramatically accelerates microbial community succession. *PloS one* **9**: e102609.

Koskineemi S, Lamoureux JG, Nikolakakis KC, de Roodenbeke CtK, Kaplan MD, Low DA *et al* (2013). Rhs proteins from diverse bacteria mediate intercellular competition. *Proceedings of the National Academy of Sciences* **110**: 7032-7037.

Lambertsson L, Nilsson M (2006). Organic material: the primary control on mercury methylation and ambient methyl mercury concentrations in estuarine sediments. *Environmental science & technology* **40**: 1822-1829.

- 659 Liu Y-R, Yu R-Q, Zheng Y-M, He J-Z (2014a). Analysis of the Microbial Community Structure
660 by Monitoring an Hg Methylation Gene (hgcA) in Paddy Soils along an Hg Gradient. *Applied*
661 *and environmental microbiology* **80**: 2874-2879.
- 662
- 663 Liu Y-R, Zheng Y-M, Zhang L-M, He J-Z (2014b). Linkage between community diversity of
664 sulfate-reducing microorganisms and methylmercury concentration in paddy soil. *Environmental*
665 *Science and Pollution Research* **21**: 1339-1348.
- 666
- 667 Lozupone C, Lladser ME, Knights D, Stombaugh J, Knight R (2011). UniFrac: an effective
668 distance metric for microbial community comparison. *The ISME journal* **5**: 169.
- 669
- 670 Lu X, Liu Y, Johs A, Zhao L, Wang T, Yang Z *et al* (2016). Anaerobic mercury methylation and
671 demethylation by *Geobacter bemidjensis* Bem. *Environmental science & technology* **50**: 4366-
672 4373.
- 673
- 674 Mahowald MA, Rey FE, Seedorf H, Turnbaugh PJ, Fulton RS, Wollam A *et al* (2009).
675 Characterizing a model human gut microbiota composed of members of its two dominant
676 bacterial phyla. *Proceedings of the National Academy of Sciences* **106**: 5859-5864.
- 677
- 678 Markowitz VM, Chen I-MA, Palaniappan K, Chu K, Szeto E, Grechkin Y *et al* (2012). IMG: the
679 integrated microbial genomes database and comparative analysis system. *Nucleic acids research*
680 **40**: D115-D122.
- 681
- 682 Martens EC, Koropatkin NM, Smith TJ, Gordon JI (2009). Complex glycan catabolism by the
683 human gut microbiota: the Bacteroidetes Sus-like paradigm. *Journal of Biological Chemistry*
684 **284**: 24673-24677.
- 685
- 686 Martini MC, Bollweg GL, Levitt MD, Savaiano DA (1987). Lactose digestion by yogurt beta-
687 galactosidase: influence of pH and microbial cell integrity. *The American journal of clinical*
688 *nutrition* **45**: 432-436.
- 689
- 690 Mcleod E, Chmura GL, Bouillon S, Salm R, Björk M, Duarte CM *et al* (2011). A blueprint for
691 blue carbon: toward an improved understanding of the role of vegetated coastal habitats in
692 sequestering CO₂. *Frontiers in Ecology and the Environment* **9**: 552-560.
- 693
- 694 Moeck GS, Coulton JW (1998). TonB - dependent iron acquisition: Mechanisms of siderophore
695 - mediated active transport. *Molecular microbiology* **28**: 675-681.
- 696
- 697 Morel FM, Kraepiel AM, Amyot M (1998). The chemical cycle and bioaccumulation of
698 mercury. *Annual review of ecology and systematics*: 543-566.
- 699
- 700 Parks JM, Johs A, Podar M, Bridou R, Hurt RA, Smith SD *et al* (2013). The genetic basis for
701 bacterial mercury methylation. *Science* **339**: 1332-1335.
- 702
- 703 Pernthaler J (2013). Freshwater microbial communities. *The Prokaryotes*. Springer. pp 97-112.
- 704

- Podar M, Gilmour CC, Brandt CC, Soren A, Brown SD, Crable BR *et al* (2015). Global prevalence and distribution of genes and microorganisms involved in mercury methylation. *Science advances* **1**: e1500675.
- Poulain AJ, Barkay T (2013). Cracking the mercury methylation code. *Science* **339**: 1280-1281.
- Ramli N, Abd-Aziz S, Hassan MA, Alitheen N, Kamaruddin K (2015). Potential cyclodextrin glycosyltransferase producer from locally isolated bacteria. *African Journal of Biotechnology* **9**: 7317-7321.
- Ravichandran M (2004). Interactions between mercury and dissolved organic matter—a review. *Chemosphere* **55**: 319-331.
- Reimers CE, Alleau Y, Bauer JE, Delaney J, Girguis PR, Schrader PS *et al* (2013). Redox effects on the microbial degradation of refractory organic matter in marine sediments. *Geochimica et Cosmochimica Acta* **121**: 582-598.
- Roy V, Amyot M, Carignan R (2009). Beaver ponds increase methylmercury concentrations in Canadian shield streams along vegetation and pond-age gradients. *Environmental science & technology* **43**: 5605-5611.
- Seibert CM, Raushel FM (2005). Structural and catalytic diversity within the amidohydrolase superfamily. *Biochemistry* **44**: 6383-6391.
- Si Y, Zou Y, Liu X, Si X, Mao J (2015). Mercury methylation coupled to iron reduction by dissimilatory iron-reducing bacteria. *Chemosphere* **122**: 206-212.
- Smith SD, Bridou R, Johs A, Parks JM, Elias DA, Hurt RA *et al* (2015). Site-directed mutagenesis of HgcA and HgcB reveals amino acid residues important for mercury methylation. *Applied and environmental microbiology* **81**: 3205-3217.
- Stackebrandt E (2014). The Emended Family Peptococcaceae and Description of the Families Desulfitobacteriaceae, Desulfotomaculaceae, and Thermincolaceae. *The Prokaryotes*. Springer. pp 285-290.
- Stegen JC, Lin X, Konopka AE, Fredrickson JK (2012). Stochastic and deterministic assembly processes in subsurface microbial communities. *The ISME journal* **6**: 1653-1664.
- Stolpovsky K, Fetzer I, Van Cappellen P, Thullner M (2016). Influence of dormancy on microbial competition under intermittent substrate supply: insights from model simulations. *FEMS microbiology ecology* **92**: fiw071.
- Tatusov RL, Fedorova ND, Jackson JD, Jacobs AR, Kiryutin B, Koonin EV *et al* (2003). The COG database: an updated version includes eukaryotes. *BMC bioinformatics* **4**: 1.

- Taylor BL, Zhulin IB (1999). PAS domains: internal sensors of oxygen, redox potential, and light. *Microbiology and Molecular Biology Reviews* **63**: 479-506.
- Taylor PG, Townsend AR (2010). Stoichiometric control of organic carbon–nitrate relationships from soils to the sea. *Nature* **464**: 1178-1181.
- Ueno A, Shimizu S, Tamamura S, Okuyama H, Naganuma T, Kaneko K (2016). Anaerobic decomposition of humic substances by *Clostridium* from the deep subsurface. *Scientific reports* **6**.
- Ullrich SM, Tanton TW, Abdrashitova SA (2001). Mercury in the aquatic environment: a review of factors affecting methylation. *Critical reviews in environmental science and technology* **31**: 241-293.
- Wang C, Chang C, Chu C, Lee D, Chang B-V, Liao C (2003). Producing hydrogen from wastewater sludge by *Clostridium bifermentans*. *Journal of Biotechnology* **102**: 83-92.
- Waples JS, Nagy KL, Aiken GR, Ryan JN (2005). Dissolution of cinnabar (HgS) in the presence of natural organic matter. *Geochimica et Cosmochimica Acta* **69**: 1575-1588.
- Wett B, Rauch W (2003). The role of inorganic carbon limitation in biological nitrogen removal of extremely ammonia concentrated wastewater. *Water Research* **37**: 1100-1110.
- Wetzel RG (1992). Gradient-dominated ecosystems: sources and regulatory functions of dissolved organic matter in freshwater ecosystems. *Dissolved organic matter in lacustrine ecosystems*. Springer. pp 181-198.
- Windham-Myers L, Marvin-DiPasquale M, Stricker CA, Agee JL, Kieu LH, Kakouros E (2014). Mercury cycling in agricultural and managed wetlands of California, USA: Experimental evidence of vegetation-driven changes in sediment biogeochemistry and methylmercury production. *Science of the Total Environment* **484**: 300-307.
- Windham - Myers L, Marvin - Dipasquale M, Krabbenhoft DP, Agee JL, Cox MH, Heredia - Middleton P *et al* (2009). Experimental removal of wetland emergent vegetation leads to decreased methylmercury production in surface sediment. *Journal of Geophysical Research: Biogeosciences (2005–2012)* **114**.
- Yeom S-J, Kim Y-S, Oh D-K (2013). Development of Novel Sugar Isomerases by Optimization of Active Sites in Phosphosugar Isomerases for Monosaccharides. *Applied and environmental microbiology* **79**: 982-988.
- Yu R-Q, Reinfelder JR, Hines ME, Barkay T (2013). Mercury methylation by the methanogen *Methanospirillum hungatei*. *Applied and environmental microbiology* **79**: 6325-6330.
- Zhao Y, Ren N, Wang A (2008). Contributions of fermentative acidogenic bacteria and sulfate-reducing bacteria to lactate degradation and sulfate reduction. *Chemosphere* **72**: 233-242.

796

797

798

Figures.

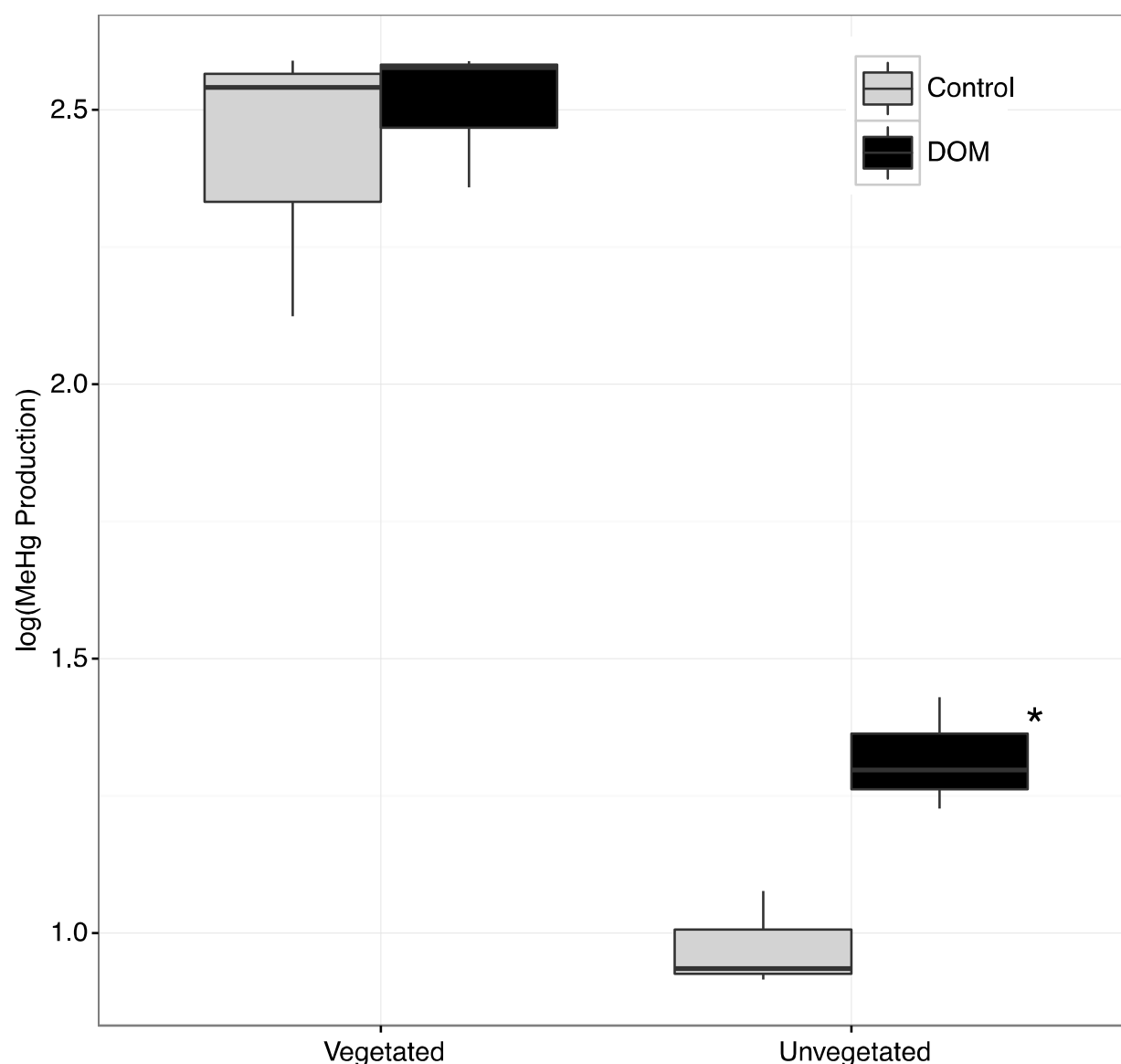


Figure 1. Boxplots are shown for methylmercury production, with upper and lower hinges representing the values at the 75th and 25th percentiles and whiskers representing 1.5 times value at the 75th and 25th percentiles, respectively. DOM did not significantly increase methylmercury production in, vegetated sediment, but induced methylmercury production in unvegetated sediment. Regardless of DOM amendment, vegetated sediment experienced an order of magnitude higher rates of mercury methylation.

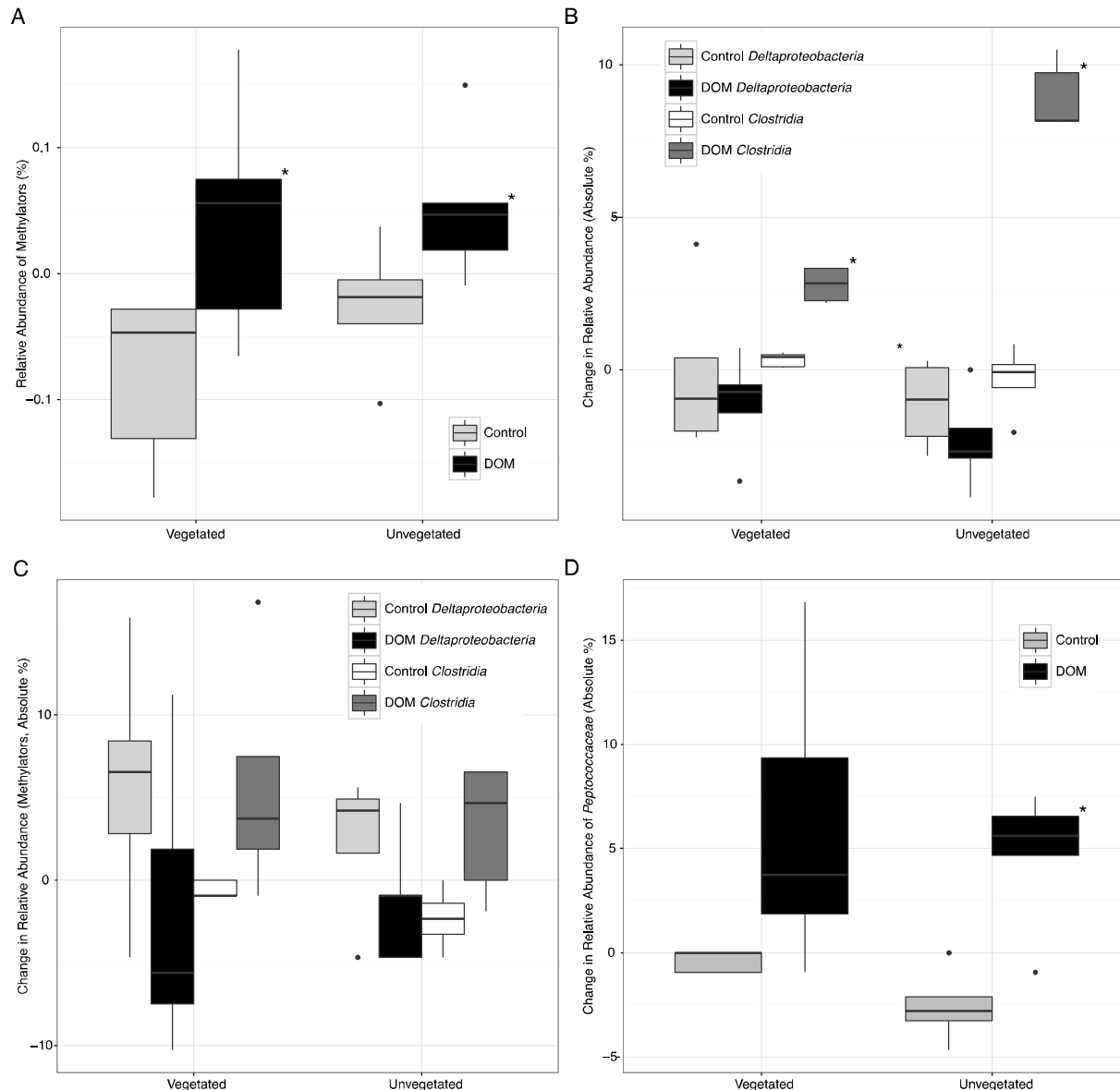


Figure 2. Boxplots are shown for selected changes in abundance of methylator abundance (A) and taxonomy (B-D) in response to DOM addition, with upper and lower hinges representing the values at the 75th and 25th percentiles and whiskers representing 1.5 times value at the 75th and 25th percentiles, respectively. Outliers are plotted as points. Shading for each bar denote taxonomy and DOM-amended vs. control. Significant relationships ($P < 0.05$) are denoted with an asterisk. (A) The relative abundance of methylating organisms increased in both sediment types in response to DOM addition. (B) The addition of DOM decreased the proportion of *Deltaproteobacteria* and increased the proportion of *Clostridia* in both vegetated and unvegetated sediment, with greater effects in unvegetated sediment. (C) Within potential methylators, *Deltaproteobacteria* decreased and *Clostridia* increased in response to DOM addition, (D) driven by changes within the family *Peptococcaceae*.

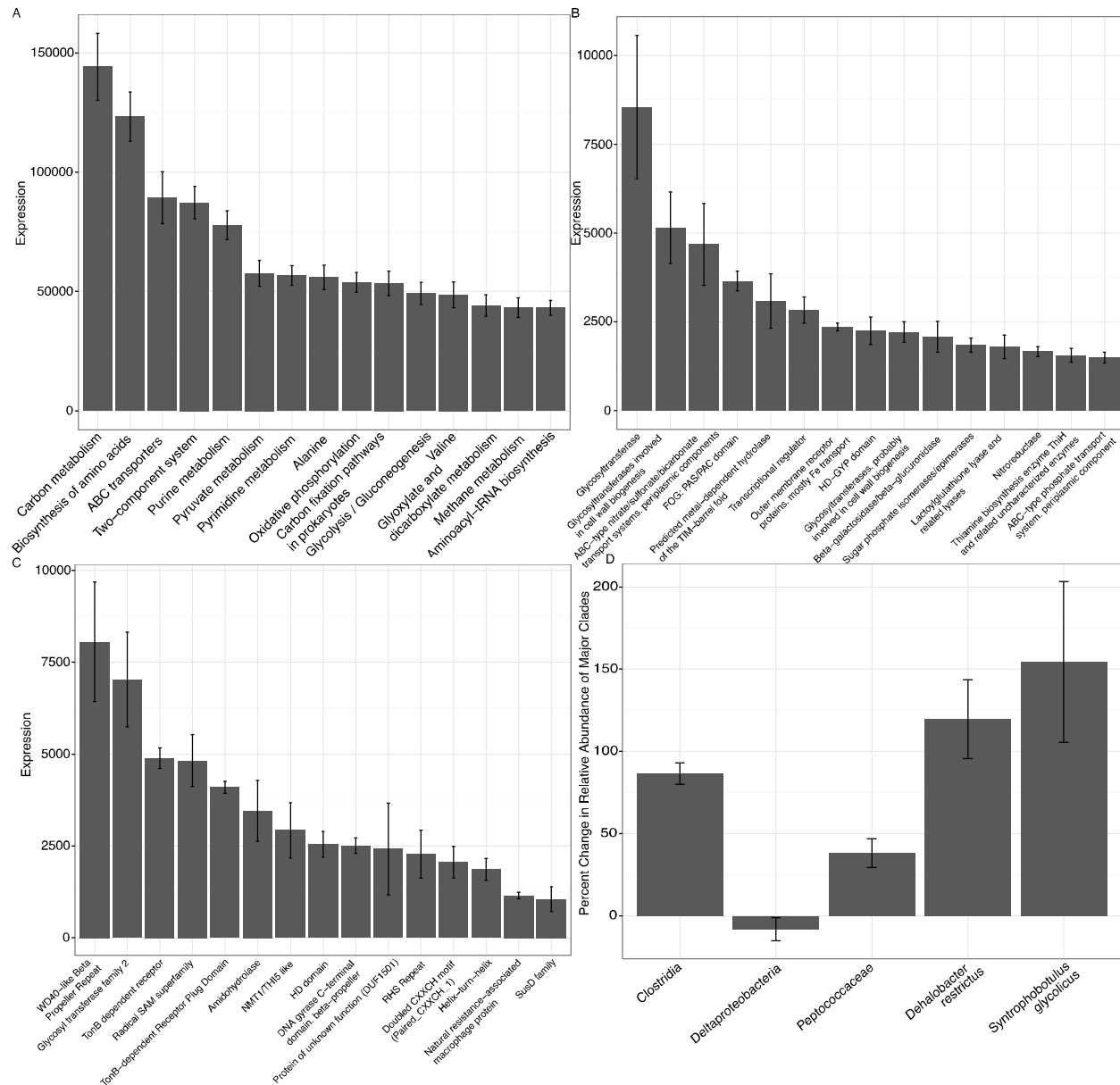


Figure 3. Results from analysis of metagenomic shotgun sequences from unvegetated microcosms are denoted in Figure 3. Panels A, B, and C show the expression of the top 15 upregulated (T4 vs. T0) KEGG, COG, and Pfam targets, respectively. Panel D shows percent change in selected taxonomic groups at T4 vs. T0.

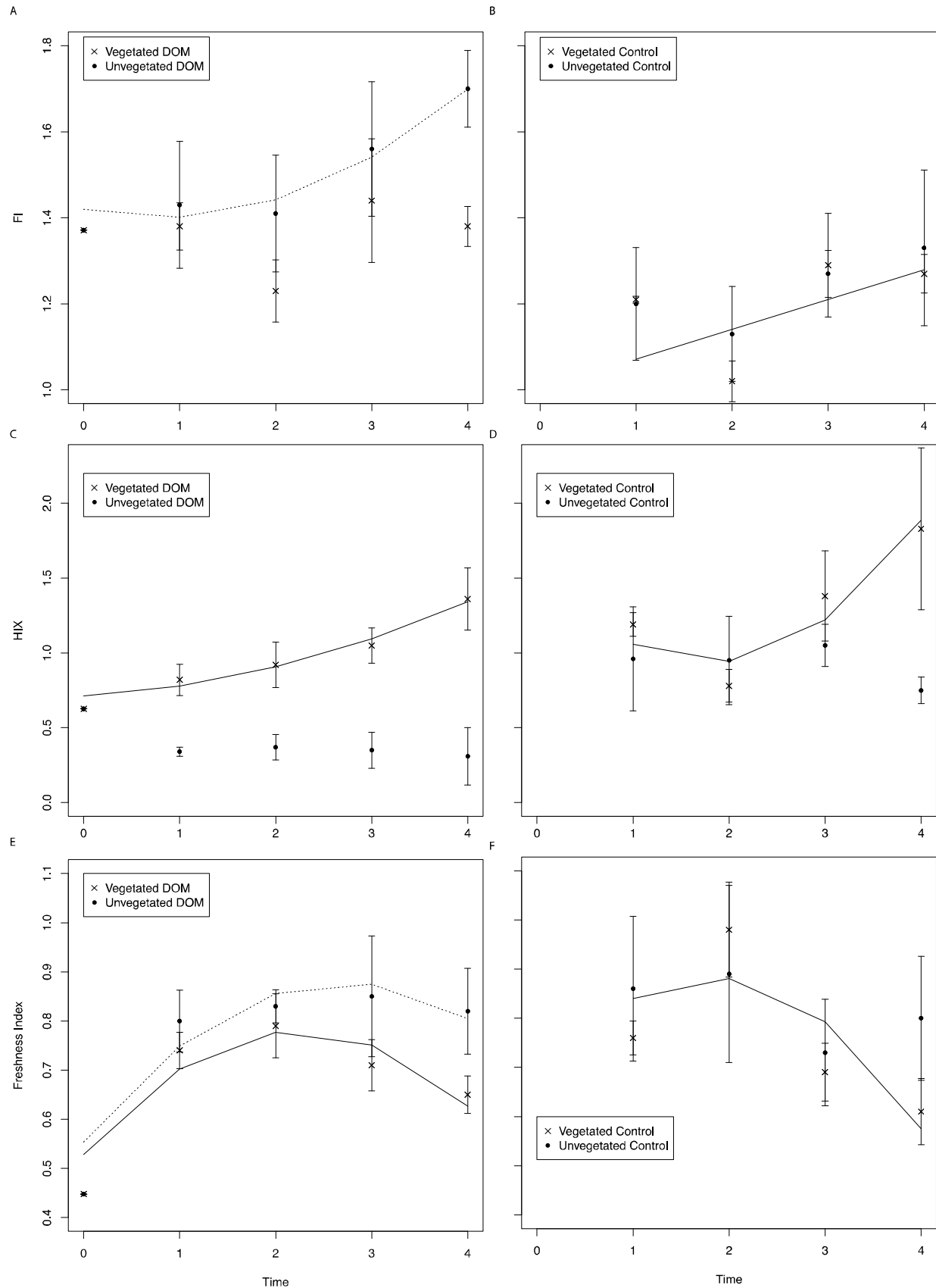


Figure 4. DOM fluorescence indices were assessed through time with linear and quadratic regressions in each environment and microcosm type. Averages for each environment and microcosm type are plotted at T0-T4, with error bars representing the standard deviation. Plots in the first column at DOM-amended microcosms, while plots in the second column are control microcosms. Unvegetated microcosms are depicted as closed circles with dashed lines showing significant regressions; vegetated microcosms are x's with solid lines showing significant regressions. (A) and (B) denote FI, (C) and (D) denote HIX, and (E) and (F) denote freshness.

Tables.

Table 1. Mean chemical and biological characteristics of vegetated and unvegetated environments are presented Table 1. Asterisks represent significant differences and standard deviations are presented in parentheses.

	Vegetated Environment	Unvegetated Environment
pH*	5.6(0.09)	5.8(0.40)
NH ₄ ⁺ (mg/L)***	1.49(0.32)	0.36(0.14)
TPOC(mg/L)***	1.13(0.06)	0.09(0.05)
TDN(mg/L)**	0.06(0.02)	0.04(0.01)
percent C***	13.16(2.20)	1.82(3.39)
percent N***	0.8(0.06)	0.1(0.23)
C:N*	16.43(1.59)	20.06(5.36)
DNA concentration(ng/L)***	28.13(5.06)	9.31(3.16)
NAG(nmol/h/g)***	308.94(81.30)	9.05(9.29)
BG(nmol/h/g)***	371.22(81.25)	17.71(19.29)
PHOS(nmol/h/g)***	393.45(55.06)	20.69(17.33)
SMHG(ng/g)**	2.67(2.18)	0.24(0.12)
STHG(ng/g)	306.56(551.07)	3.16(3.99)
SM/THG	0.02(0.009)	0.32(0.45)
Proteobacteria***	0.3(0.04)	0.43(0.02)
Chloroflexi***	0.17(0.01)	0.06(0.009)
Bacteroidetes	0.11(0.02)	0.13(0.03)
Acidobacteria*	0.07(0.009)	0.08(0.02)
Nitrospirae***	0.05(0.009)	0.02(0.009)
Actinobacteria***	0.03(0.007)	0.07(0.01)
Alpha Diversity*	116.73(6.65)	120.6(11.33)

* $P \leq 0.10$

** $P \leq 0.05$

*** $P \leq 0.01$

Table 2. R^2 values from regression analysis of changes in DOM properties through time are listed in Table 2. Control microcosms were analyzed from T1-T4 and DOM-amended microcosms were analyzed from T0-T4, with characteristics of the applied DOM represented at T0.

	NPOC (mg/L)	Total Fluorescence	Fluor:NPOC	FI	HIX	Freshness
Vegetated, Control (T1-T4)	0.39**	0.21*	n.s.	0.22**	0.51***	0.52***
Vegetated, DOM-amended (T0-T4)	0.32***	n.s.	n.s.	n.s.	0.68****	0.57***
Unvegetated, Control (T1-T4)	0.64****	n.s.	0.29**	n.s.	n.s.	n.s.
Unvegetated, DOM-amended (T0-T4)	n.s.	n.s.	n.s.	0.41***	n.s.	0.39***

* $P \leq 0.10$

** $P \leq 0.05$

*** $P \leq 0.01$

**** $P \leq 0.001$

Table 3. Pearson's Correlation was used to assess relationships of selected upregulated COG and Pfam targets with HIX and MeHg production at T4 ($n = 3$). Relationships are presented in Table 3.

	HIX	MeHg
COG		
Glycosyltransferase	0.98*	0.79
Glycosyltransferases involved in cell wall biogenesis	0.96*	0.76
ABC-type nitrate/sulfonate/bicarbonate transport systems, periplasmic components	-0.85	0.55
FOG/PAS/PAC domain	-0.88	0.60
Predicted metal-dependent hydrolase of the TIM-barrel fold	0.88	0.60
Transcriptional regulator	0.999**	0.88
Outer membrane receptor proteins, mostly Fe transport	-0.79	0.45
HD-GYP domain	0.99**	0.84
Glycosyltransferases, probably involved in cell wall biogenesis	0.96*	0.74
Beta-galactosidase/beta-glucuronidase	0.98*	-0.80
Sugar phosphate isomerases/epimerases	-0.73	0.36
Lactoylglutathione lyase and related lyases	-0.93	0.67
Nitroreductase	0.996**	0.86
Thiamine biosynthesis enzyme ThiH and related uncharacterized enzymes	0.98*	0.80
ABC-type phosphate transport system, periplasmic component	-0.66	0.27
Pfam		
WD40-like beta propeller repeat	0.99**	0.85
Glycosyltransferase family 2	0.97*	0.76
TonB-dependent receptor	0.90	0.999***
Radical SAM superfamily	0.95*	0.75
TonB-dependent receptor plug domain	0.51	-0.83
Amidohydrolase	-0.87	0.57
NMT1/THI5 like	-0.87	0.58
HD domain	0.9997**	0.91
DNA gyrase C-terminal domain, beta-propeller	-0.94	0.70
Protein of unknown function (DUF1501)	-0.46	0.04
RHS repeat	-0.80	0.46
Doubled CXXCH motif (Paired_CXXCH_1)	0.97*	0.78
Helix-turn-helix	-0.90	0.63
Natural resistance-associated macrophage protein	-0.83	0.51
SusD family	0.99*	-0.82

* $P < 0.10$ ** $P < 0.05$